Draft version January 13, 2014
Preprint typeset using LaTeX style emulateapj v. 04/03/99

arXiv:astro-ph/0303370v2 31 Mar 2003

EXTERNAL SHOCK MODEL FOR THE LARGE-SCALE, RELATIVISTIC X-RAY JETS FROM THE MICROQUASAR XTE J1550-564

X. Y. Wang, Z. G. Dai and T. Lu
Department of Astronomy, Nanjing University, Nanjing 210093, P.R.China

Draft version January 13, 2014

ABSTRACT

Large-scale, decelerating, relativistic X-ray jets due to material ejected from the black-hole candidate X-ray transient and microquasar XTE J1550-564 has been recently discovered with *Chandra* by Corbel et al. (2002). We find that the dynamical evolution of the eastern jet at the late time is consistent with the well-known Sedov evolutionary phase. A trans-relativistic external shock dynamic model by analogy with the evolution of gamma-ray burst remnants, is shown to be able to fit the observation data reasonably well. The inferred interstellar medium density around the source is well below the canonical value $n_{\rm ISM} \sim 1$ cm^{-3}. We find that the emission from the continuously shocked interstellar medium (forward shock region) decays too slowly to be a viable mechanism for the eastern X-ray jet. However, the rapidly fading X-ray emission can be interpreted as synchrotron radiation from the non-thermal electrons in the adiabatically expanding ejecta. These electrons were accelerated by the reverse shock (moving back into the ejecta) which becomes important when the inertia of the swept external matter leads to an appreciable slowing down of the original ejecta. To ensure the dominance of the emission from the shocked ejecta over that from the forward shock region during the period of the observations, the magnetic field and electron energy fractions in the forward shock region must be far below equipartition. Future continuous, follow-up multi-wavelength observations of new ejection events from microquasars up to the significant deceleration phase should provide more valuable insight into the nature of the interaction between the jets and external medium.

Subject headings: stars:individual (XTE J1550-564)— gamma rays: bursts—ISM: jets and outflows— radiation mechanisms: non-thermal

1. INTRODUCTION

Black-hole X-ray binaries with relativistic jets resemble, on a much smaller scale, many of the phenomena seen in quasars and are therefore called microquasars (Mirabel & Radriguez 1999). Apparently superluminal radio jets are observed from at least the two best known microquasars GRS 1915+105 (Mirabel & Rodriguez 1994; Fender et al. 1999) and GRO J1655-40 (Tingay et al. 1995; Hijellming & Rupen 1995), with the actual jet velocities greater than 0.9c. Their motions are consistent with being purely ballistic, up to a projected separation of 0.08pc from the compact object on a maximum time scale of 4 months after the ejection for GRS 1915+105. With the help of *Chandra* Observatory, Corbel et al. (2002) recently discovered large-scale (with projected separation more than a half pc from the compact object), relativistically moving and decelerating radio and X-ray emitting jets from the microquasar XTE J1550-564. It is the first time that an X-ray jet proper-motion measurements spanning several years are obtained for accretion-powered Galactic sources. Hence, XTE J1550-564 provides a good opportunity to study the dynamical evolution of relativistic jets.

In this paper, we propose that the dynamical evolution and radiation of the large-scale X-ray jets from XTE J1550-564 can be understood as the interaction between the jet and the surrounding interstellar medium (ISM), quite similar to the external shock model for afterglows of gamma-ray bursts (GRBs) (Rees & Mészáros 1992; Mészáros & Rees 1997). The main differences lie in the initial Lorentz factor and the kinetic energy of the jets. The microquasar jets are inferred to be at least mildly relativistic with initial Lorentz factor $\Gamma_0 \sim 2-5$ (Mirabel & Radriguez 1999)[1], in contrast to the ultra-relativistic jets ($\Gamma_0 > 100$) in GRBs. When the relativistic ejecta from the microquasar is significantly decelerated by the ISM, a relativistic *forward* shock expands into the ISM and a *reverse* shock moves into and heats the original ejecta. The shocked ambient and ejecta materials are in pressure balance and separated by a contact discontinuity. The forward shock continuously heats fresh ISM and accelerates electrons, while the reverse shock operates only once and after that the shocked gas in the ejecta expands and cools adiabatically. As more and more ISM matter are swept-up, the ejecta and the shocked ISM — we shall call them 'jet'— should be decelerated more and more and finally transit to the non-relativistic motion phase. We find that this dynamic model can fit well the observed proper-motion evolution of the large scale eastern X-ray jet from XTE J1550-564.

In both shocks, the kinetic energy are converted to the internal energy. In the standard theory of GRB afterglows, it is assumed that shocked electrons and the magnetic field acquire constant fractions of the total shock energy, denoted by ϵ_e and ϵ_B for electrons and magnetic field respectively. The inferred values from a few afterglows are in the range: $\epsilon_e \simeq 0.1-0.6$ and $\epsilon_B \simeq 10^{-6}-0.1$ (e.g. Granot et al. 1999; Wijers & Galama 1999; Panaitescu & Kumar

[1]Recently, Fender (2003) argued that the two-sided jet proper motions observed from microquasars can only allow placing lower limits on the initial Lorentz factors.

2002). If we assume that the same processes also occur in the large-scale, decelerating jet we consider here, we are able to know the emission from the forward shock and reverse shock regions. We find that forward shock emission decays too slowly to be consistent with the X-ray emission from the eastern jet of XTE J1550-564, but the emission from the post-shocked adiabatically expanding ejecta can give a reasonable fit.

First, we give a brief review of the observations of the large scale jets from XTE J1550-564 in section 2. We present the dynamic model fit in section 3 and interpret the radiation in section 4. Finally, we give conclusions and discussions.

2. OBSERVATIONS OF THE LARGE-SCALE JETS FROM XTE J1550-564

The X-ray transient XTE J1550-564 was discovered by the All-Sky Monitor on aborad the *Rossi X-ray Timing Explorer* on 7 September 1998 (Smith 1998). Optical observations of the source in quiescence showed that the mass of the compact object is near $10M_{\odot}$, indicating that the compact object is a black hole and revealed that the binary companion to be low-mass star (Hannikainen et al. 2001). The distance (d) to the source is constrained to be in the range 2.8-7.6 kpc with a favored value of 5.3 kpc (Orosz et al. 2002). Soon after the discovery of the source, an extremely strong X-ray flare was observed on 20 September 1998 (Sobczak et al. 2000; Homan et al. 2001), and radio jets with apparent superluminal velocities (the initial proper motion was greater than 57 mas day^{-1}) was observed beginning 24 September 1998 (Hannikainen et al. 2001). During the 2002 X-ray outburst, radio observations were made with the *Australia Telescope Compact Array (ATCA)*. The detection of the large-scale radio jet $\sim$ 22 arcsec to the west of XTE J1550-564 led to a re-analysis of the archival *Chandra* data and discovery of an X-ray jet to the east of XTE J1550-564 (Corbel et al. 2002; Tomsick et al. 2003). It is thought that both jets are connected with the 20 September 1998 ejection event, based on the detection of superluminal jets following an extremely large X-ray flare and the absence of any other X-ray flare of similar magnitude in continual X-ray monitoring from 1996 to 2002.

According to the archival *Chandra* data, the field of view of XTE J1550-564 was imaged by *Chandra* on 9 June, 21 August, and 11 September 2000. These observations present for the first time the proper-motion measurement for an X-ray jet from microquasars, which show direct evidence for gradual deceleration. Radio observations with ATCA show a decaying and moving radio source consistent with the position of the eastern X-ray jet. Remarkably, the overall radio flux detected on 1 June 2002 for the eastern jet is consistent with an extrapolation of the X-ray spectrum with a single power law of spectral index of $\alpha \simeq -0.6$ ($F_\nu \propto \nu^\alpha$) (Tomsick et al. 2003), which provides evidence for a synchrotron X-ray emission mechanism[2]. The field of view of XTE J1550-564 was further observed by *Chandra* on 11 March 2002. We summarize the observations for both the eastern and western jets in Table 1.

For the western jet, Kaaret et al. (2003) also examined the archival *Chandra* data on XTE J1550-564 at June, August and September 2000, but found no evidence for X-ray emission in any of the archival observations with an upper bound on the absorbed flux of 1.1×10^{-14}ergcm^{-2}s^{-1}. The facts that no X-ray emission detected from the western jet during 2000 and that the eastern source apparently moves faster than the western one are consistent with the interpretation in which the eastern jet is the approaching one and the western jet is the receding one. The brightening of the western jet at the late time argues against symmetric jet propagation and may reflect the non-uniformity in the ISM.

3. THE DYNAMIC MODEL

As we only know the proper motion measurements and the light curve of the eastern jet, we focus on modelling the dynamical evolution and radiation of this jet.

We envision a beamed outflow with kinetic energy E_0 and Lorentz factor Γ_0 ejected from the microquasar XTE J1550-564 expands conically with a half opening angle θ_j into the ambient medium with a constant number density n. The interaction between the relativistic ejecta and the surrounding medium is analogous to GRB external shock, but with quite different E_0 and Γ_0. The supersonic motion of the ejecta should drive a blast wave propagating into the ISM. We shall assume that the radiation loss of the shock wave is a negligible fraction of the total energy, so the dynamic is adiabatic throughout. From the view of the energy conservation, the dynamic equation can be simplified as (see also Huang, Dai & Lu 1999)

$$(\Gamma-1)M_0c^2+\sigma(\Gamma_{\rm sh}^2-1)m_{\rm sw}c^2=E_0, \qquad (1)$$

where Γ and $\Gamma_{\rm sh}$ are the Lorentz factors of the jet material and the shock front respectively, $m_{\rm sw} = (4/3)\pi R^3 m_p n(\theta_j^2/4)$ is the mass of the swept-up ISM (where R is the shock radius, m_p is the mass of the proton) and M_0 is the mass of the original ejecta. The first term on the left of the equation is the kinetic energy of the ejecta and the second term is the internal energy of the shock. For ultra-relativistic shocks $\sigma = 6/17$, while $\sigma = 0.73$ for non-relativistic shocks (Blandford & Mckee 1976) [3]. For simplicity, we approximate this term as $0.7(\Gamma^2-1)m_{\rm sw}c^2$ in the following calculation (Note that at observation time the jet has transited to the sub-relativistic motion phase and that a slight difference of σ may reflect it in the value of E_0, which is a free parameter here).

The kinematic equation of the approaching jet is

$$\frac{dR}{dt}=\frac{\beta(\Gamma)c}{1-\beta(\Gamma)\cos\theta}, \qquad (2)$$

where $v=\beta c$ is the bulk velocity of the jet with $\beta(\Gamma) = (1-\Gamma^{-2})^{1/2}$, t is the observer time and θ is the jet inclination angle to the line of sight.

Given the initial condition at $t = 0$, which is chosen to be $R_0 = 10^7$cm and $\Gamma_0 = 3$, the two equations can be solved and we can get the relation between the proper motion μ ($\mu = R\sin\theta/d = R\sin\theta/5.3$kpc) and time t.

[2]The broadband spectral energy distribution of the western jet around 11 March 2002, which is consistent with a single power law of spectral index of -0.660 ± 0.005, strengthened the synchrotron radiation origin of the X-ray emission (Corbel et al. 2002) .

[3]Strictly speaking, these values are corresponding to point explosions with shock structure described by the similarity solution.

We find that the following combination of the parameters fits the observed proper-motion data reasonably well: $E_0 = 3.6 \times 10^{44}$erg, $n = 1.5 \times 10^{-4}\mathrm{cm}^{-3}$, $\theta_j = 1.5^\circ$ and $\theta = 50^\circ$.[4] The model fit is plotted in Figure 1 as the solid line. The late time behavior approaches the well-known Sedov solution $R \propto t^{2/5}$ (see the dashed line in Fig. 1). This is expected since the second term on the left of Eq.(1) becomes dominant at the late time, so $\beta^2 R^3 =$ constant. In addition, $\frac{dR}{dt} \simeq \beta c$ when $\beta\cos\theta \ll 1$. The earlier phase can be regarded as the transition regime from the mildly relativistic motion to the non-relativistic motion. By comparison, we also plot the $R \propto t^{0.5}$ and $R \propto t^{0.3}$ cases in Figure 2, which show clear deviations from the data.

The inferred value of the ISM density is surprisingly low. Such low densities with $n \lesssim 10^{-3}\mathrm{cm}^{-3}$ have been inferred around another two microquasars GRS 1915+105 and GRO J1655-40 by Heinz (2002) from the fact that jets move with constant velocities up to distance $\gtrsim 0.04$ pc. As argued by Heinz (2002), this implies that either the sources are located in regions occupied by the hot ISM phase or previous activities of the jets have created evacuated bubbles around the sources.

4. THE RADIATION MODEL

4.1. *The forward shock emission*

First, we try to fit the X-ray emission of the eastern jet using the forward shock model, the mechanism believed to be responsible for GRB afterglows. In the standard picture of GRBs, an afterglow is generally believed to be produced by the synchrotron radiation or inverse Compton emission of the shock-accelerated electrons in an ultra-relativistic shock wave expanding into the ambient medium. As more and more ambient matter is swept up, the shock gradually decelerates while the emission from such a shock fades down. The microquasar jet is similar to the GRB remnant at the time that its Lorentz factor has decreased to $\Gamma \sim 1-3$, usually months to years after the burst. So, we expect that similar emission processes should also occur in the case of the microquasar decelerating jet.

If the distribution of the shock-accelerated electrons takes a power-law form with the number density given by $n(\gamma_e)d\gamma_e = K\gamma_e^{-p}d\gamma_e$ for $\gamma_m < \gamma_e < \gamma_M$, the volume emissivity at the frequency ν' in the comoving frame of the shocked gas is (Rybicki & Lightman 1979)

$$j_{\nu'} = \frac{\sqrt{3}q^3}{2m_e c^2}\left(\frac{4\pi m_e c\nu'}{3q}\right)^{\frac{1-p}{2}} B_\perp^{\frac{p+1}{2}} K F_1(\nu', \nu'_m, \nu'_M), \quad (3)$$

where q and m_e are respectively the charge and mass of the electron, $B_\perp$ is the strength of the component of magnetic field perpendicular to the electron velocity, ν'_m and ν'_M are the characteristic frequencies for electrons with γ_m and γ_M respectively, and

$$F_1(\nu', \nu'_m, \nu'_M) = \int_{\nu'/\nu'_M}^{\nu'/\nu'_m} F(x) x^{(p-3)/2} dx \quad (4)$$

with $F(x) = x\int_x^{+\infty} K_{5/3}(t)dt$ ($K_{5/3}(t)$ is the Bessel function).

The physical quantities in the pre-shock and post-shock ISM are connected by the jump conditions:

$$n' = \frac{\hat{\gamma}\Gamma + 1}{\hat{\gamma} - 1} n, \quad e' = \frac{\hat{\gamma}\Gamma + 1}{\hat{\gamma} - 1}(\Gamma - 1) n m_p c^2, \quad (5)$$

$$\Gamma_{\rm sh}^2 = \frac{(\Gamma + 1)[\hat{\gamma}(\Gamma - 1) + 1]^2}{\hat{\gamma}(2 - \hat{\gamma})(\Gamma - 1) + 2}, \quad (6)$$

where e' and n' are the energy and the number densities of the shocked gas in its comoving frame and $\hat{\gamma}$ is the adiabatic index, which equals 4/3 for ultra-relativistic shocks and 5/3 for sub-relativistic shocks. A simple interpolation between these two limits $\hat{\gamma} = (4\Gamma + 1)/3\Gamma$ gives a valid approximation for trans-relativistic shocks (Dai, Huang & Lu 1999).

Assuming that shocked electrons and the magnetic field acquire constant fractions (ϵ_e and ϵ_B) of the total shock energy, we get

$$\gamma_m = \epsilon_e \frac{p-2}{p-1}\frac{m_p}{m_e}(\Gamma - 1), B_\perp = \sqrt{8\pi\epsilon_B e'} \quad (7)$$

and

$$K = (p-1) n' \gamma_m^{p-1} \quad (8)$$

for $p > 2$.[5] It is reasonable to believe that ν'_M is well above the X-ray band throughout the observations, because the forward shock continuously heats fresh ISM and accelerates electrons. The observer frequency ν relates to the frequency ν' in the comoving frame by $\nu = D\nu'$, where $D = 1/\Gamma(1 - \beta\cos\theta)$ is the Doppler factor. The observed flux density at ν and the X-ray flux in the band 0.3-8keV are respectively given by

$$F_\nu = \frac{\theta_j^2}{4}\left(\frac{R}{d}\right)^2 \Delta R D^3 j_{\nu'}; \quad F(0.3-8\mathrm{keV}) = \int_{\nu_1}^{\nu_2} F_\nu d\nu, \quad (9)$$

where ΔR is the width of the shock region and is assumed to be $\Delta R = R/10$ in the calculation. The model fit to the light curve of the eastern jet is presented in Figure 3. Clearly, the model light curve decays too slowly to fit the observed data. This is expected from the following analytic study. For $\nu'_m \ll \nu' \ll \nu'_M$, $F_\nu \propto D^3 B_\perp^{(p+1)/2} K R^3 \propto D^3 B_\perp^{(p+1)/2} n' \gamma_m^{p-1} R^3$. When $\beta \ll 1$, $\beta \propto t^{-3/5}$, $R \propto t^{2/5}$, $B \propto \beta$, $\gamma_m \propto \beta^2$ and $n' = 4n =$ constant. So, we get $F_\nu \propto t^{-(15p-21)/10} \propto t^{-1.2}$ for $p = 2.2$. We also consider the case in which the jet spreads laterally with the sound velocity as discussed in GRBs(Rhoads 1999), but find that it makes little difference.

4.2. *The reverse shock emission*

Another probable emitting region for X-rays is the adiabatically expanding ejecta itself. A reverse shock wave that moves back through the original ejecta becomes important when the swept-up matter mass equals $1/\Gamma_0$ of the ejecta mass. The reverse shock accelerates electrons in the ejecta and may amplify the original magnetic field to be close to equipartition. The emission from the non-thermal ($N(\gamma_e) \propto \gamma_e^{-p}$) relativistic electrons in the adiabatically

[4] $\theta = 50^\circ$ and $\Gamma_0 = 3$ are consistent with the initial proper motion > 57 mas day^{-1} for $d = 5.3$kpc.

[5] The expressions of γ_m and K are different if $p < 2$ (see e.g. Dai & Cheng 2001).

expanding ejecta with radius R is described by the van der Laan (1966) model, where the flux density is given by $F_\nu \propto R^{-2p}\nu^{(1-p)/2}$ in the optically-thin regime. So, when $\beta \ll 1$, $F_\nu \propto t^{-4p/5} \propto t^{-1.76}$ for $p = 2.2$. This decay is still too slow to fit the observed light curve of the X-ray jet for which the power-law fit gives a decay index of -3.7 ± 0.7 (Kaaret et al. 2003). However, different from the continuous forward shock, the reverse shock operates only once, so the electrons, including those with the maximum energy in the ejecta, all cool adiabatically. So it is likely that, at some time, the characteristic frequency of the electrons with the maximum energy $\gamma_M m_e c^2$ may fall close to the X-ray band and the X-ray flux would decay quite rapidly since then.

The maximum energy of the power-law distribution electrons just after the reverse shock crosses the ejecta is determined by the shock acceleration process, which is however not well understood. If the electrons in the high energy end of the power law cool faster than the dynamical time scale, the real maximum energy of the electrons in the ejecta is limited by the synchrotron cooling timescale; electrons with energy greater than this energy would have cooled down within the dynamical timescale. So, $E_M^0 = \min(E_{M,acc}, E_{M,cool})$, where $E_{M,acc}$ and $E_{M,cool}$ denote the maximum energies allowed by the shock acceleration process and the cooling process respectively, the superscript 0 in E_M^0 denotes the value at t_0— the time when the reverse shock heats the ejecta. If the synchrotron radiation dominates the cooling of the electrons, $E_{M,cool} = 6\pi m_e^2 c^3/(\sigma_T B_\perp^2 t_0')$, where $t_0' = t_0/D(t_0)$ is the dynamical time in the comoving frame, $D(t_0)$ is the Doppler factor of the X-ray jet at the time t_0, σ_T is the Thomson cross section.

The physical quantities in the adiabatically expanding ejecta with radius R relate with their initial value at t_0 by (van der Laan 1966)

$$\gamma_m = \gamma_m(t_0)\frac{R_0}{R}, \qquad \gamma_M = \gamma_M(t_0)\frac{R_0}{R}; \tag{10}$$

$$K = K(t_0)\left(\frac{R}{R_0}\right)^{-(2+p)}, B_\perp = B_\perp(t_0)\left(\frac{R}{R_0}\right)^{-2} \tag{11}$$

if the synchrotron emission cooling is negligible, where R_0 is the radius of the ejecta at time t_0 and $\gamma_M(t_0) = E_M^0/m_e c^2$. These relations are derived from the assumption that total number of the electrons is conserved and that the magnetic field is frozen to the plasma fluid[6].

From the dynamic model in section 3, we get $t_0 = 121$ days and $R_0 = 0.71\times10^{18}$cm for the eastern X-ray jet from XTE J1550-564. Given the initial condition for $K(t_0)$, $B_\perp(t_0)$, $\gamma_m(t_0)$ and $\gamma_M(t_0)$, we can obtain the model light curves of the emissions from the expanding ejecta using Eqs.(3), (4), (9) and $R(t)$. In the calculation, we have assumed $\gamma_M(t_0) = E_{M,cool}/m_e c^2 = 6\pi m_e c/(\sigma_T B_\perp(t_0)^2 t_0')$. We find that the following combination of the initial values can fit the flux data well (see Figure 4): $B_\perp(t_0) = 0.5$ mG and $K(t_0) = 0.8$ cm^{-3} and $\gamma_m(t_0) = 100$.[7] For these values, $\gamma_M(t_0) = 3.55 \times 10^8$.

Noting that $K = \epsilon_e(p-2)e'\gamma_m^{p-2}$ and $B_\perp = \sqrt{8\pi\epsilon_B e'}$, the above value for $K(t_0)$ and $B_\perp(t_0)$ imply that the equipartition parameters for energies in electrons and magnetic field in the reverse shock are $\epsilon_e = 0.6$ and $\epsilon_B = 0.44\times10^{-2}$ respectively, if the internal energy density in the reverse shock is equal to that in the forward shock region at time t_0. Surprisingly, these equipartition values are close to the typical values inferred for GRB afterglows (Granot et al. 1999, Wijers & Galama 1999; Wang, Dai & Lu 2000). Please also note that here the emitting electrons are in slow cooling regime as $\nu_m(t_0) \sim 10^7$Hz $\ll \nu_c$, where ν_c is the cooling frequency, and that at the X-ray band the synchrotron emission dominates over the inverse Compton emission (Sari & Esin 2001; Panaitescu & Kumar 2000).

We further calculate the model spectrum for the eastern jet on 1 June 2000 using the above parameter values and plot the fit of the observed data in Figure 5. Clearly the model fits quite well the energy spectrum on 1 June 2000, 621 days after the ejection of the eastern jet from XTE J1550-564. At this time, the characteristic frequency of the electrons with γ_M is just near the X-ray band, so the X-ray spectrum doesn't become steeper. The model predicts that there should be significant steepness of X-ray spectrum at March 2002, but the relatively few counts do not give a reliable spectral index (Kaaret et al. 2003).

We have shown that the emission from the shocked ejecta provides a viable mechanism for the rapidly decaying X-ray flux from the eastern jet of XTE J1550-564. To guarantee the dominance of the emission from the shocked ejecta over that from the forward shock region during the period of the observations, the forward shock emission should be below the upper limit of the observation made on June 19 2002. Fig.3 tells us that the forward shock emission for $\epsilon_e = 0.1$ and $\epsilon_B = 10^{-4}$ is inferred to be below the limit. Because $F_\nu \propto \gamma_m^{p-1}B^{(p+1)/2} \propto \epsilon_e^{p-1}\epsilon_B^{(p+1)/4}$, the magnetic field and electron energy fractions in the forward shock region must satisfy (see Fig. 3)

$$\left(\frac{\epsilon_e}{0.1}\right)^{p-1}\left(\frac{\epsilon_B}{10^{-4}}\right)^{(p+1)/4} \lesssim 1. \tag{12}$$

The high value for ϵ_B in the reverse shock region relative to that in the forward shock region can be accounted for if the ejecta has already been magnetized before the further shock compression[8]. This is reasonable as the ejecta from microquasars are suggested to originate from the inner accretion disks (Mirabel & Rodriguez 1999). A pair-rich outflow from the microquasar probably account for the comparatively large value of ϵ_e in the reverse shock. Future observations of large-scale jets from microquasars may provide better understanding of the shock physics and physical condition in relativistic jets.

5. CONCLUSIONS AND DISCUSSIONS

It is believed that relativistic jets exist in accreting systems ranging from Galactic X-ray binaries, gamma-ray

[6]The same relation for the magnetic field holds if we assume that the energy in the magnetic field constitutes a constant fraction of the internal energy in the ejecta during the whole adiabatically expanding phase.

[7]The model result is very insensitive to the value of $\gamma_m(t_0)$

[8]The high value of ϵ_B inferred for GRB afterglows can, however, be attributed to particular environment (e.g. Königl & Granot 2002) around the burst or a particular magnetic field amplification mechanism (e.g. Thompson & Madau 2000).

bursts and active galactic nuclei (AGNs). Jets in Galactic X-ray binaries such as XTEJ1550-564 evolves much more rapidly than AGN jets and therefore offer a good opportunity to study the dynamical evolution of relativistic jets on time scales inaccessible for AGNs. Although afterglows in GRBs evolves also rapidly, their cosmological distances make the direct measurements of the proper-motion impossible and their dynamics can be studies only indirectly.

The discovery of the extended radio and X-ray emission from the microquasar XTE J550-564 (Corber et al. 2002; Tomsick et al. 2003; Kaaret et al. 2003) represents the first detection of large-scale relativistic jets from a Galactic black hole candidate in both radio and X-rays. These large-scale jets appear to arise from a relatively brief ejection event and, therefore, offer a unique opportunity to study the large-scale evolution of an impulsive jet. We find that the dynamical evolution of the observed eastern jet from the XTE J550-564 is consistent with the well-known Sedov evolutionary phase, during which the energy in the jet is conserved and $R \propto t^{2/5}$. The apparent superluminal motion observed at the very early epoch implies that the initial motion of the jet is at least mildly relativistic. As more and more ISM matter is swept up, the jet decelerates and finally transits to the non-relativistic phase. A trans-relativistic external shock dynamical model is shown to be able to fit the observed proper motion data reasonably well. The inferred ISM density around the jet is $n \sim 1.5 \times 10^{-4}\mathrm{cm}^{-3}$, well below the canonical value. Such low ISM density gains support from the inferred value $n \lesssim 10^{-3}\mathrm{cm}^{-3}$ around another two microquasars GRS 1915+105 and GRO J1655-40 by Heinz (2002), from the fact that jets move with constant velocities (i.e. no slowing down) up to distance $\gtrsim 0.04$ pc. As suggested by Heinz (2002), this implies either that the sources are located in regions occupied by the hot ISM phase or that previous frequent activities of the jets have created evacuated bubbles around the sources.

We first try to fit the X-ray light curve of the eastern jet with the emission from the shocked ISM. However, it is found that this predicts a decay too slow to fit the observations. The model predicts $F_\nu \propto t^{-(15p-21)/10} \sim t^{-1.2}$ during the non-relativistic phase, while the power law fit of the X-ray flux data gives $F_\nu \propto t^{-3.7\pm0.7}$ (Kaaret et al. 2003). We then turn to another likely emission region—the adiabatically expanding ejecta heated by the reverse shock, quite similar to the mechanism suggested to be responsible for the optical flash and radio flare from GRB990123 (Sari & Piran 1999). Different from the shocked ISM, all electrons in the ejecta cool by adiabatic expansion, so the maximum energy of the electrons in the ejecta decreases as well[9]. Once the characteristic synchrotron radiation frequency of these electrons falls close to the X-ray band, the X-ray flux from the ejecta should decay quite rapidly (drops exponentially with time) since then. Using this model, we fitted both the X-ray light curve data and the energy spectrum on 1 June 2000 of the eastern jet successfully (see Figures 4 and 5). One prediction we can make here is a flattening of the light curve at late time, once the forward shock emission, if still above the detection limit, overtakes the reverse shock emission.

The western (receding) jet from XTE J1550-564 was detected in radio and X-rays in 2002 while archival *Chandra* data on this source from June, August and September 2000 only give upper limits. The non-detection in 2000 is consistent with the deduction that the western source is the receding jet. Unlike the smoothly decaying eastern jet, the western jet brightens at the late time. The brightening might be caused by the inhomogeneities in the ISM (Kaaret et al. 2003) or internal shocks produced by a faster jet overtaking a slower one (Kaiser et al. 2000), and need further careful study. The western jet moved by 0.52 ± 0.13 arc sec between 11 March and 19 June 2002 with a mean apparent speed significantly less than the average apparent speed from 1998 to early 2002. Interestingly, we find that the decay of the X-ray flux of the western jet between March and June 2002 is also consistent with that predicted by the reverse shock emission $F_\nu \propto t^{-4/5p} \propto t^{-1.86}$ for $p = 2.32$ of the western jet.

Besides the relativistically moving, decelerating jets from XTE J1550-564, large-scale X-ray jets and radio lobes up to ~ 40 arcmin size have been observed from SS433 (Brinkmann et al. 1996; Dubner et al. 1998). The radiation is suggested to come from the termination shock which results from the interaction of the mass outflow with the nebula W50. Recently, reheating of baryonic material in X-ray jets of SS433 is inferred to take place within $\sim 10^{17}$cm from the core, based on the observed iron emission lines (Migliari, Fender & Méndez 2002). We think that external shock is a possible mechanism for such reheating. As suggested for TeV neutrino emission from microquasar jets (through internal shocks) by Levinson & Waxman (2002), external shocks of microquasar jets may also accelerate the protons in both the shocked ISM and the shocked ejecta. So, they are also potential sources of cosmic-rays (Heinz & Sunyaev 2002), high-energy neutrinos and high-energy gamma-rays.

In summary, we developed a model for the dynamical evolution and radiation of the large-scale X-ray jets from the microquasar XTE J1550-564 analogous to the external shock model for GRB afterglows. In this model, the observed jet emission is due to interaction between the jets and external ISM. Future continuous, follow-up multi-wavelength observations of new ejection events from microqusasrs up to the significant deceleration phase should provide more valuable insights into the nature and physical condition (e.g. shock and particle acceleration physics) of relativistic jets. Owing to the proximity of the Galactic X-ray binaries, further studies on them also offer an exciting way for a better understanding of relativistic jets seen elsewhere in the Universe.

We are grateful to the anonymous referee for his/her valuable suggestions. This work was supported by the National Natural Science Foundation of China under grants 19973003, 19825109 and 10233010, and the National 973 project.

[9]However, for the forward shock, there are always new electrons being shocked. γ_M is determined by the balance between the acceleration timescale and the cooling timescale: $\gamma_M \propto B^{-1/2}$ (e.g. Mészáros et al. 1993) . So, for the forward shock, γ_M even increases with time, since the magnetic field decreases with time.

REFERENCES

Blandford, R. D. & Mckee, C. F. 1976, Phys. Fluids, 19, 1130
Brinkmann, W., Aschenbach, B., Kawai, N., 1996, A&A, 312, 306
Corbel, S., Fender, R., Tzioumis, A. K., et al., 2002, Science, 298, 196.
Dai, Z. G., Huang, Y. F. & Lu, T., 1999, ApJ, 520, 634
Dai, Z. G. & Cheng, K. S. , 2001, ApJ, 558, L109
Dubner, G. M., Holdaway, M., Goss, W. M., Mirabel, I. F., 1998, AJ, 116, 1842
Fender, R. et al. 1999, MNRAS, 304, 865
Fender, R. 2003, MNRAS, accepted, astro-ph/0301225
Granot, J., Piran, T., Sari, R., 1999, ApJ, 527, 236
Hannikainen, D., et al., 2001, ApSS, 276, 45
Heinz, S. 2002, A&A, 388, L40
Heinz, S., Sunyaev, R., 2002, A&A, 390, 751
Hijellming, R. M. & Rupen, M. P., 1995, Nature, 375, 464
Homan, J., et al., 2001, ApJS, 132, 377
Huang, Y. F., Dai, Z. G. & Lu, T., 1999, MNRAS, 309, 513
Kaaret, P., Corbel, S., Tomsick, J. A., et al., 2003, ApJ, 582, 945
Kaiser, C. R., Sunyaev, R., Spruit, H. C., 2000, A&A, 356, 975
Königl, A. & Granot, J., 2002, ApJ, 574, 134
Levinson, A. & Waxman, E., 2002, Phys. Rev. Lett. 87, L101
Mészáros, P., Laguna, P. & Rees, M. J., 1993, ApJ, 405, 278
Mészáros, P. & Rees, M. J., 1997, ApJ, 476, 232
Migliari, S., Fender, R., Méndez, 2002, Science, 297, 1673
Mirabel, I. F. & Rodriguez, L. F., 1994, Nature, 371, 46
Mirabel, I. F. & Rodriguez, L. F., 1999, ARA&A, 37, 409
Orosz, J. A., et al., 2002, ApJ, 568, 845.
Panaitescu, A.& Kumar, P., 2000, ApJ, 543, 66
Panaitescu, A.& Kumar, P., 2002, ApJ, 571, 779
Rees, M. J. & Mészáros, P. 1992, MNRAS, 258, P41
Rhoads, J. E., 1999, ApJ, 525, 737
Rybicki, G. B. & Lightman, A. P., 1979, Radiative Process in Astrophysics (New York: Wiley).
Sari, R. & Piran, T. 1999, ApJ, 517, L109
Sari, R. & Esin, A. A., 2001, ApJ, 548, 787
Smith, D. A., 1998, IAU Circ. No 7008.
Sobczak, G. J., et al., 2000, ApJ, 544, 993
Thompson, C. & Madau, P., 2000, ApJ, 538, 105
Tingay, S. J., 1995, Nature, 374, 141
Tomsick, J. A., Corbel, S., Fender, R., et al., 2003, ApJ, 582, 933
van der Laan, H., 1966, Nature, 211, 1131
Wang, X. Y., Dai, Z. G. & Lu, T., 2000, MNRAS, 319, 1159
Wijers, R. A. M. J., & Galama, T. J., 1999, ApJ, 523, 177

TABLE 1
ANGULAR SEPARATIONS AND THE ABSORBED X-RAY FLUX OF THE EASTERN AND WESTERN JETS

Date	Time after X-ray flare (days)	Angular Separation (arcsec)		Flux (10^{-14}ergcm^{-2}s^{-1})	
		eastern jet	western jet	eastern jet	western jet
June 9 2000	628	21.3 ± 0.5		20 ± 6	< 1.1
Aug. 21 2000	700	22.7 ± 0.5		6.1 ± 1.3	< 1.1
Sept. 11 2000	720	23.4 ± 0.5		8.2 ± 1.5	< 1.1
Mar. 11 2002	1265	29.0 ± 0.5	~ 23	1.1 ± 0.3	19 ± 1.0
June 19 2002	1335		$\sim 23+$ 0.52 ± 0.13	$< 0.3 \pm 0.2$	16 ± 1.0

References.— Corbel et al. 2002; Kaaret et al. 2003; Tomsick et al. 2003

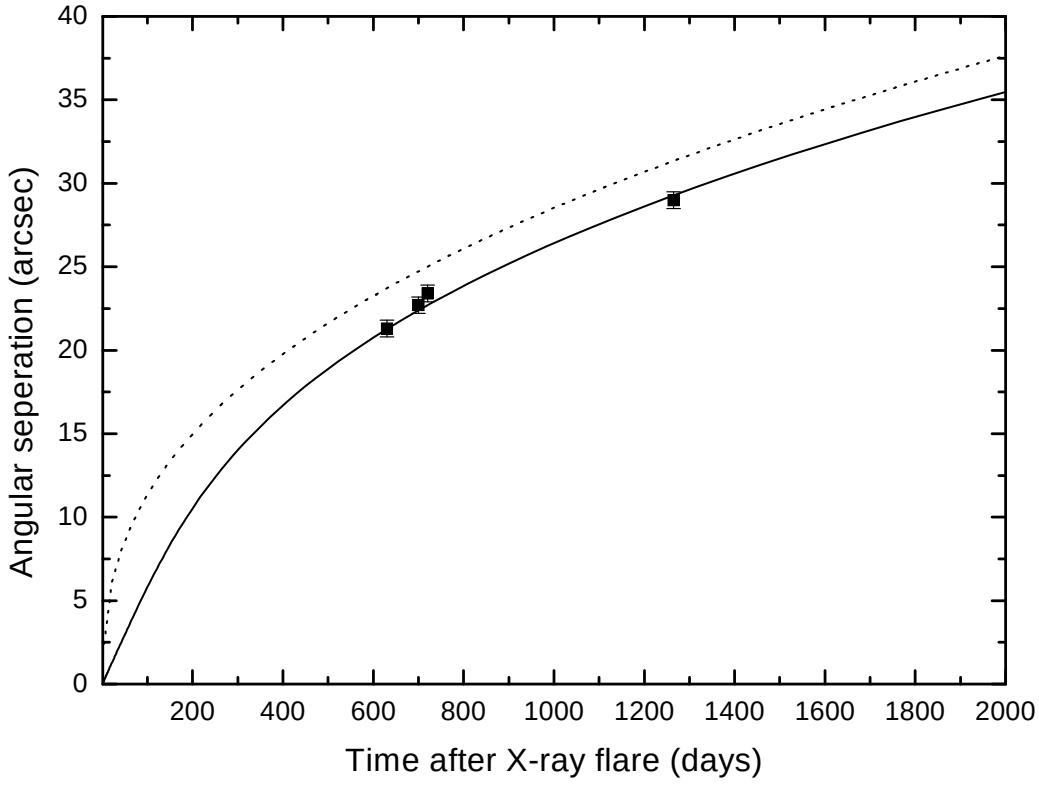


FIG. 1.— Model fit to the position of the eastern X-ray jet verse time. Observation data are taken from Tomsick et al. (2003) and Kaaret et al. (2003). The solid line is the fit in terms of the trans-relativistic external shock model. We also plot the function $R \propto t^{2/5}$ (dotted line) for comparison.

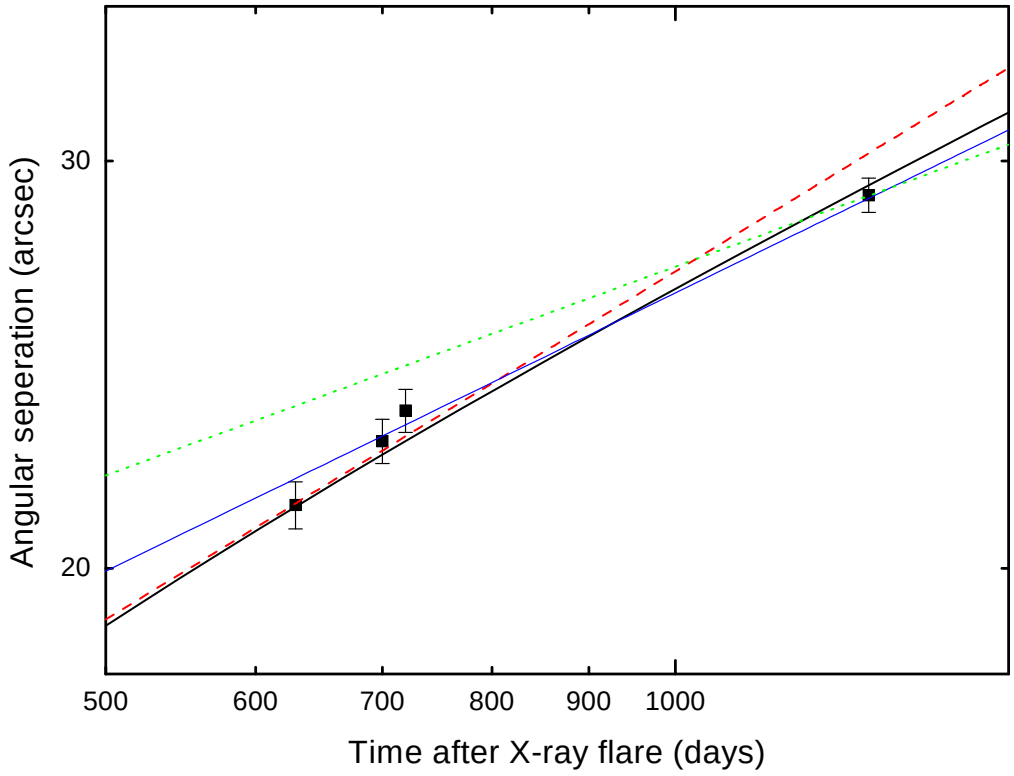


FIG. 2.— Comparison of the model fits for the position of the eastern X-ray jet verse time. The thick solid line is the tran-relativistic external shock model developed in this paper. The (blue) thin solid line, (green) dotted line and (red) dashed line represent $R \propto t^{0.4}$, $R \propto t^{0.3}$, $R \propto t^{0.5}$ respectively. It shows that the dynamical evolution of the eastern jet is consistent with the Sedov evolutionary phase $R \propto t^{0.4}$ at the late time.

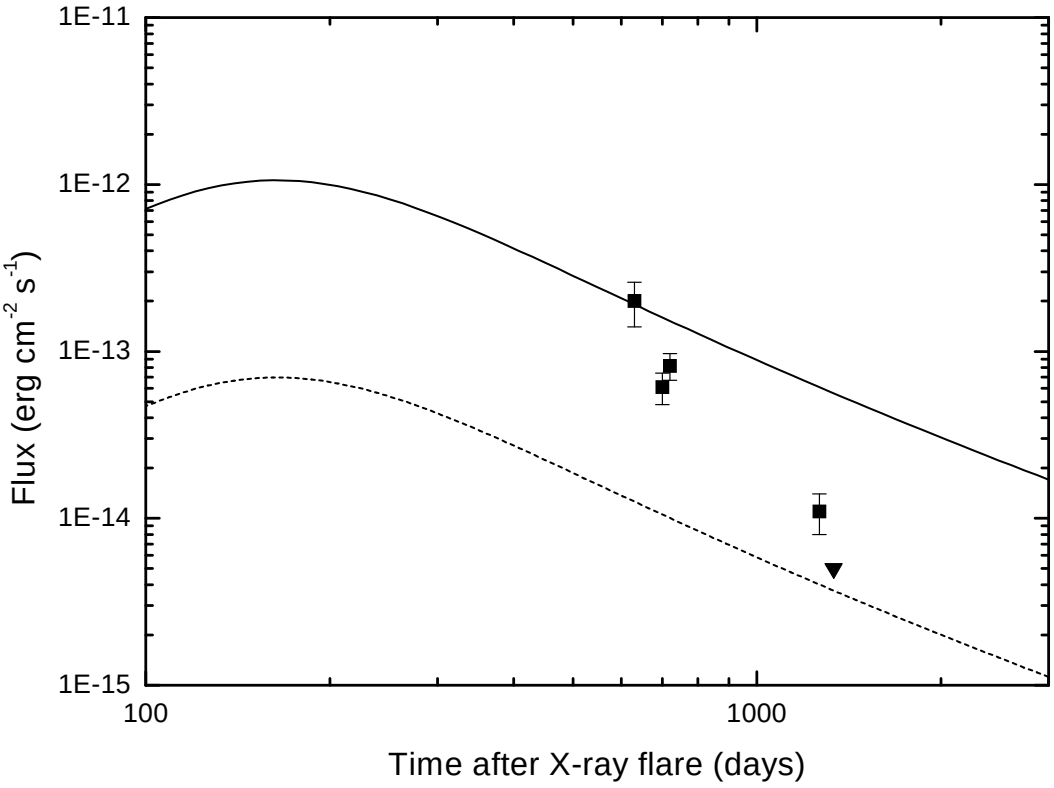


FIG. 3.— Model and observed X-ray light curves of the eastern jet. Detections and upper limits for the non-detections, taken from Tomsick et al. (2003) and Kaaret et al. (2003), are indicated by the filled squares and arrows respectively. The solid line and dotted line represent X-ray emission from the shocked ISM (forward shock) with different electron (ϵ_e) and magnetic field (ϵ_B) equipartition factors used. The solid and dotted lines are corresponding to $\epsilon_e = 0.1$, $\epsilon_B = 0.004$ and $\epsilon_e = 0.1$, $\epsilon_B = 10^{-4}$, respectively. This figure shows that the forward shock emission decays too slowly to fit the observations.

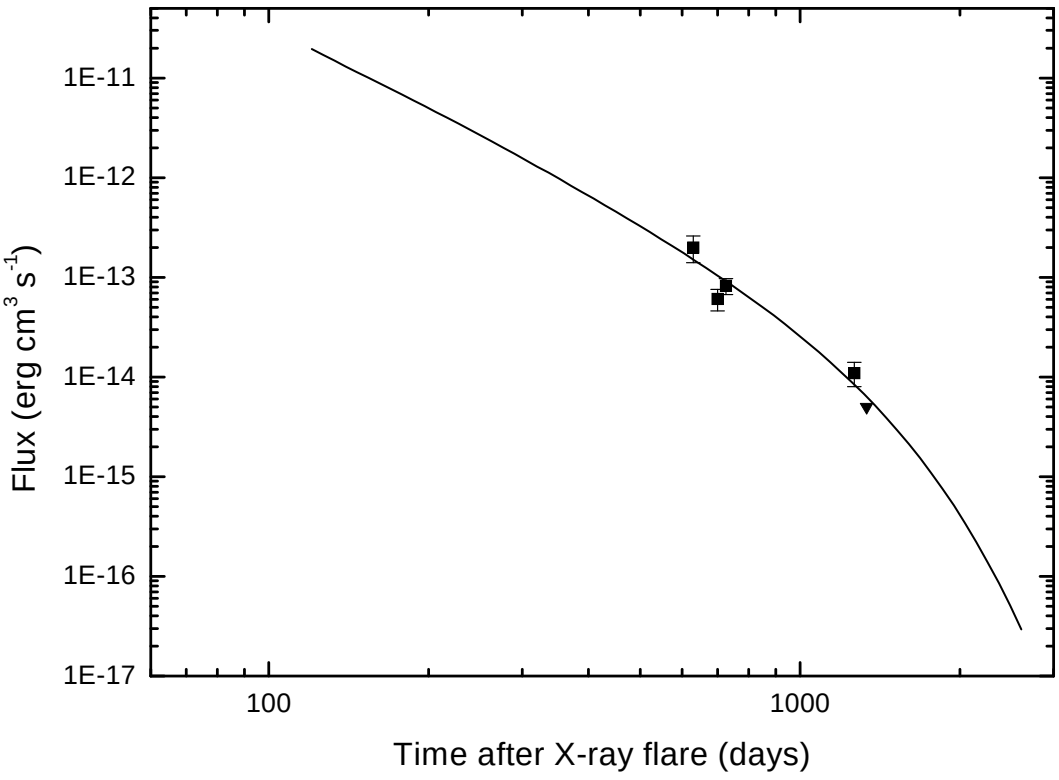


FIG. 4.— Model fit to the X-ray light curve using the synchrotron radiation from the adiabatically expanding ejecta heated by the reverse shock.

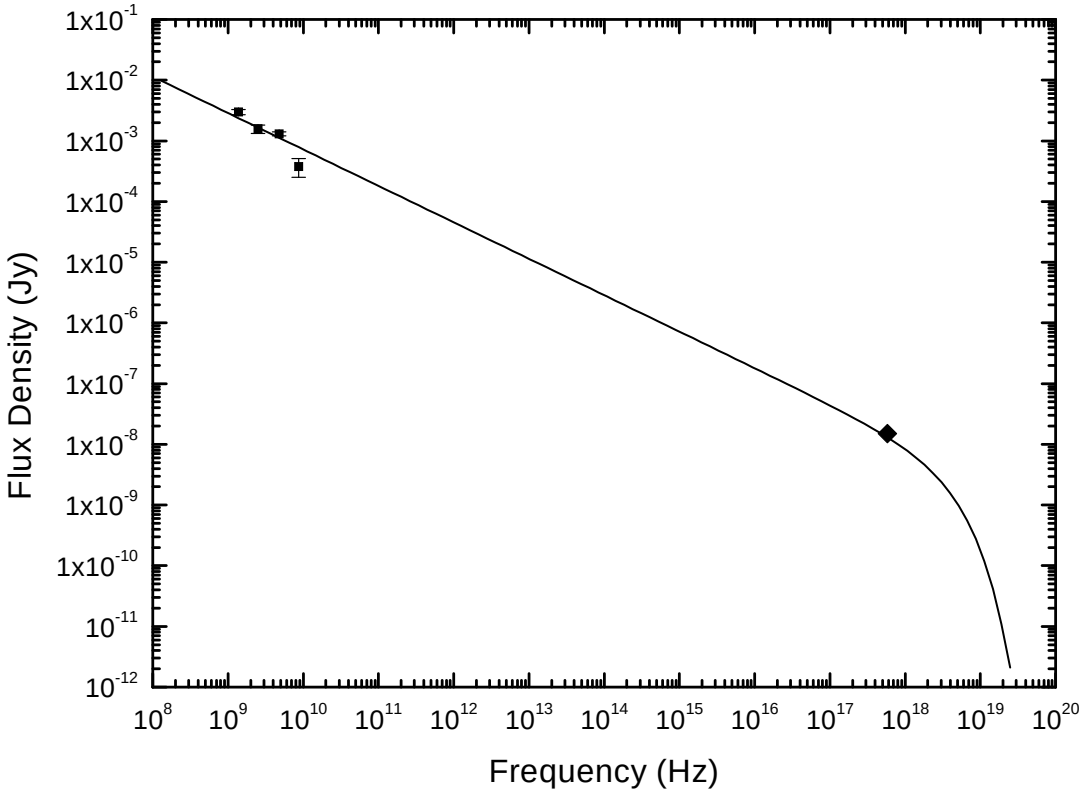


FIG. 5.— Model fit to the broadband spectrum of the eastern jet on 1 June 2000 using the synchrotron radiation from the adiabatically expanding ejecta heated by the reverse shock.